(Received 15 September 2023, Accepted 15 November 2023, Scheduled 5 December 2023)

Radio Frequency Energy Harvesting Device at ISM Band for Low Power IoT

Jefferson Ribadeneira-Ramírez*, Jorge Santamaria, Patricio Romero, and Mario Alejandro Paguay

Escuela Superior Politecnica de Chimborazo, Ecuador

ABSTRACT: Low Energy (LE) devices for communication systems like Bluetooth, 5G New Radio (NR), etc. are most likely to be powered by a battery; however, the limitation of the utilization time of this power supply entails it to be handled in different ways; one of them is using electromagnetic energy harvesting paradigm, which could be capable to supply the energy consumption of this device. In this research, the design and implementation of a device are presented for radio frequency energy harvesting in the Industrial, Scientific and Medical (ISM) band. As the first step, field intensity measurements in "Facultad de Informatica y Electronica" (FIE) were performed by the utilization of NARDA SRM 3006 radiation meter, with the aim of determining the technology with the highest radio frequency (RF) energy within the 2.4 GHz ISM band. After the analysis, WiFi technology is chosen due to the massive implementation that exists in the surroundings. Therefore, the frequency of 2.45 GHz was selected as the center frequency for the design. The device was implemented using FR4 Epoxy glass material with a dielectric permittivity of 4.4 and a dielectric thickness of 1.6 mm. The device consists of 3 stages: i) Capturing energy using a microstrip patch antenna ii) Rectification using a coupling network followed by a rectifying circuit, and iii) Energy storage using the method of harmonic balance and electromagnetic moment. Finally, harvesting measurements were carried out in FIE's laboratory; the RF energy of a WiFi router was harvested; at 10 cm a voltage of 510.6 mV was obtained, and this level of voltage was capable of turning on a led diode demonstrating the functioning of the device.

1. INTRODUCTION

Over the time, human being has had the need of different sources of energy to carry out their activities. There are different sources of energy such as solar, wind, thermal energy among others, which have been used to produce electricity. This concept is where energy harvesting (EH) comes from, which consists of taking advantage of different sources of energy from the environment and capturing a part of this energy to be stored or used directly to power different types of devices. The study of new methods that allow the utilization of renewable energies is very important for the sustainability of our planet. The fast spreading of wireless networks, Internet of Things devices, low-power consumer electronics, and sensor networks have caused the increasing use of batteries, leading to serious problems in the future, because they have a limited lifetime.

Energy harvesting systems are a burgeoning field of technology that holds great promise in our ever-growing demand for sustainable and efficient energy sources. These systems are designed to capture and convert ambient energy from the surrounding environment into usable electrical power. As we continue to face challenges related to energy generation, consumption, and environmental impact, energy harvesting systems offer innovative solutions that can reduce our reliance on traditional power sources and contribute to a more sustainable future [1]. The concept behind energy harvesting is to harness energy from sources such as sunlight, mechanical vibrations, heat differentials, or even radio waves, and convert them into electrical energy that can be stored or used to power various electronic devices and systems. These systems have the potential to revolutionize a wide range of applications, from powering remote sensors in the Internet of Things (IoT) to extending the battery life of mobile devices and reducing the environmental footprint of our technology. In this sense, RF Energy Harvesting Systems are defined as systems formed by a series of stages that aims to capture the energy from radio frequency (RF) waves present in the environment, such as radio emissions, television, mobile communications technologies such as GSM, UMTS, LTE, among other services that can be used due to their high availability [3], for example industrial, scientific and medical radio bands known as ISM, including Wi-Fi [6].

The history of RF energy harvesting started in the late 1950s where a system that captured electromagnetic waves was tested by William C. Brown, who invented and patented the term rectenna, demonstrating its operation by powering a scaled helicopter [2]. The function of a rectenna is performed by the antenna and a rectification stage that is responsible for the conversion of radio frequency energy present in the environment to direct current used to power a final device that has the characteristics of low power consumption [7]. In 1973 Glaser patented the SPS (Solar Power Satellite) system, the idea of this project was to make use of geostationary satellites as a power plant, which by means of solar panels would capture solar energy and convert it into microwaves to later be sent to earth [5]. With the idea patented by Glaser, in 1997 NASA proposed the idea of a project called Solar Tower, and the idea is to deploy a structure

* Corresponding author: Jefferson Ribadeneira-Ramírez (jefferson.Ribadeneira@espoch.edu.ec).

containing a series of solar panels in the form of a row, which are connected to an antenna responsible for transmitting energy as 5.8 GHz microwave waves, towards a series of antennas located on Earth to capture and convert it into usable energy; it is thought that this project will be launched by 2030 [5]. Currently, the use of wireless networks is increasing, which also means the increase of the electromagnetic radiation present in the environment, along with the increase in the occupation of the electromagnetic spectrum. Different wireless technologies emit a certain amount of electromagnetic energy to the environment, but part of this energy is not used in its entirety, and for this reason, the concept of RF energy harvesting or radio frequency energy harvesting becomes important [2]. In this sense, RF energy harvesting systems use a rectenna to capture energy and pass it from an AC electromagnetic waves signal to a DC signal.

Rectenna is a nonlinear device type because its structure uses a diode. This device is composed of a series of stages, starting with a receiving antenna, impedance adaptation, an RF to DC conversion stage, and an energy storage stage [8]. Its operation consists of capturing the radio frequency energy by means of a receiving antenna to be later sent to the signal rectification stage, and in the middle of these stages there is an impedance adaptation circuit used to couple both the structures, followed by a rectifier circuit and an energy storage stage [4]. The rectification stage aims to convert the signal from AC-type RF source to a continuous DC signal. One of the commonly used rectifier elements in this stage is Schottky diodes, because of their low threshold voltage and fast switching times [9]. Two groups of rectifiers can be found, half-wave and full-wave rectifiers. Half-wave rectifiers are used to eliminate part of the signal that enters either the positive (direct polarized diode) or negative part of the signal (reverse polarized diode). Gull wave rectifiers are the most common, and its operation consists of passing the negative part of the signal to positive one and vice versa, obtaining a DC signal similar to that of a battery. They give a solution to the drawbacks of half wave rectifiers, taking advantage of the total incoming wave which means both positive and negative semicycles [10].

Since the antenna and rectifier could be uncoupled, an impedance matching network takes place as a stage which is capable to ensure the maximum transmission of power [8]. It is an element that allows adapting the impedance between the source and the load to ensure the maximum energy transfer. In RF energy harvesting systems, the receiver antenna is considered as the source and the rectification stage as the load, and these adaptation networks allow to avoid the reflection loss during transmission [11]. There are several ways to implement them, but commonly 3 types of networks are defined: L-type, T-type, and n-type networks [12]. Finally, there are several factors that can introduce losses in the circuits used for RF energy harvesting, which must be considered in their design. The losses that affect the efficiency of the RF energy collection circuits are [13].

- Threshold voltage: it is the activation voltage necessary for the diode to enter its conduction state, if the voltage entering the diode is not greater than the threshold voltage, the diode will not conduct, causing the rectifier circuit to not work.
- Impedance matching: if an impedance matching network is not used between the rectifier circuit and the antenna, part of the energy captured by the antenna is reflected, causing considerable energy losses.
- Parasitic components: certain electronic components have associated intrinsic losses due to elements such as resistance, capacitance, and inductance that the devices may have.
- Harmonics: when using diodes in the rectifier circuit, they are nonlinear type and produce incident power harmonic frequencies that can reduce the amount of energy that is converted into DC [9].

From the literature, some examples related to present research can be mentioned. Ref. [18] presents a rectenna to harvest RF energy at the ISM band of 2.4 GHz prototyped on a Rogers 4003C substrate. Measurement results indicate that the proposed rectenna delivers 5.1 mW to the load. In [19], the antenna performs in the frequency band of 2.41–2.47 GHz which covers almost all channels of 2.4 GHz wireless LAN band. The simulated return loss of proposed antenna is below −10 dB, and the simulated gain is over 5 dBi. Finally, in [20] a rectenna system implemented for radio frequency energy harvesting at 2.4 GHz Bluetooth/WLAN is designed on a rectangular patch having four slots etched on the radiator providing a gain of 4.12 dBi. In this paper, a complete energy harvesting system for the ISM band is presented, which is capable to deliver the power of 51.2 mW to the load.

The rest of the paper is structured as follows. Section 2 presents the methodology focused on the analysis of the spectrum to find the center frequency for the EH device, the design and simulation of the antenna based in parameters as frequency, permittivity and permeability, the design of the rectifier to convert the input RF waves to DC voltage, a coupling network to avoid reflection losses, and finally an energy storage stage. Section 3 shows the results of all stages, and Section I4 concludes the paper.

2. METHODOLOGY

The methodology followed is presented in two sections. First, the methodology for the field strength measurements in the ISM bands is introduced. Then, the methodology followed in the design and simulation of the device for RF energy harvesting is presented.

2.1. Field Strength Measurements in the ISM Bands

To determine and analyze the opportunity of harvesting the radio frequency energy available in the environment, a measurement campaign was carried out in the ISM bands using the NARDA SRM 3006 radiation meter, which operates from 27 MHz to 3 GHz, and an isotropic three-axis E-field antenna, with the objective of select an operating frequency for the RF energy harvesting device. The procedure used to perform field

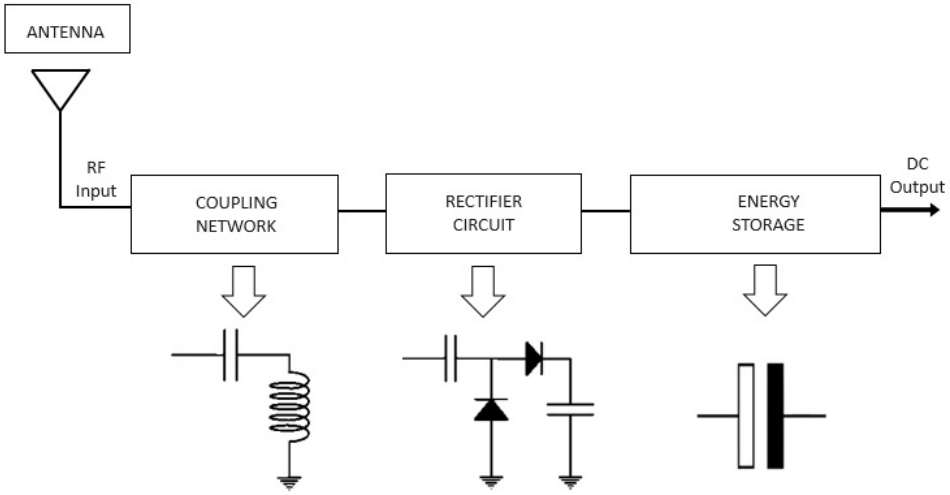

FIGURE 1. Device block diagram.

TABLE 1. ISM measured bands.

Frequency Band (MHz)	Central Frequency (MHz)	Frequency Use
26.957–27.283	27.120	Global
40.66–40.70	40.68	Global
433.05–434.79	433.92	Region 1
2400–2500	2450	Global

strength measurements starts with the study and identification of the ISM bands, measurement points, and the selection of the operating frequency.

ISM frequency bands are dispersed from 6.78 MHz to 245 GHz, which is defined in the Radio Regulations according to ITU-R in 5.138, 5.150 and 5.280 [17]. The use of these bands is given by regions and can change according to the regulations of each country. Usually within these bands, there are low-power and short-range communications systems such as wireless phones, Bluetooth devices, wireless networks, NFC, and other technologies [8]. The ISM bands in which measurements were carried out are shown in Table 1.

There are a large number of technologies that operate in the ISM bands, including the most common bands, 900 MHz band, 2.4 GHz band, and 5.8 GHz band. Some examples of technologies that operate in these bands are wireless personal area networks such as Bluetooth that works in the 2.4 GHz ISM band, wireless sensor networks, WLANs, wireless phones that can be found in the 915 MHz and 2.450 GHz bands and others such as RFID in the most common 13.56 MHz band [15].

To evaluate the field strength received in different places of the faculty of computer science and electronics, measurements were carried out at eleven different points. The aim is to observe the results and consider the different variations of field strength according to the location and surrounding environment in the different ISM bands mentioned. From these data, the design frequency of the device was determined. The results of the measurements showed that the 2.4 GHz ISM band is the one with the highest field intensity available for radio frequency energy harvesting. In this way, the study is focused on the 2.4 GHz ISM band, specifically on the 2.45 GHz frequency. This band has a bandwidth of 83.5 MHz; its range is from 2.4 GHz to 2.5 GHz; some technologies in this band are 802.11b/g/n networks, Bluetooth, wireless phones, among others. One of the most predominant technologies within this band is Wi-Fi, which usually operates on channels 1, 6, and 11 because they do not overlap.

2.2. Design and Simulation of the Device for Rf Energy Harvesting

The design of the device is based on the scheme shown in Fig. 1, in which the antenna is responsible for receiving radio frequency energy; the coupling network allows the maximum amount of power to be transferred between the antenna and the rectifier circuit, and the rectifier allows to convert the AC signal captured by the antenna into DC, to be later stored and delivered to a load or to a low energy consumption device. Each one of the stages wwa designed and simulated, starting with the microstrip patch antenna and followed by the rectifier circuit, where the coupling network stage and energy storage stages were included.

There is a wide variety of dielectric substrates used in the manufacture of microstrip antennas. It is important to compare the different materials and recognize their differences in order to select the material that provides the highest performance, in

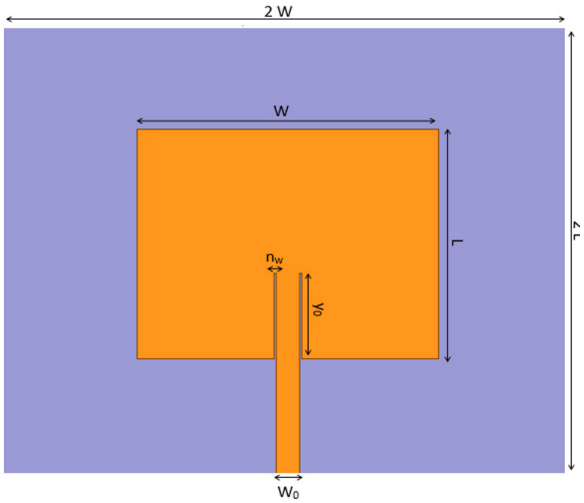

FIGURE 2. Microstrip antenna patch design.

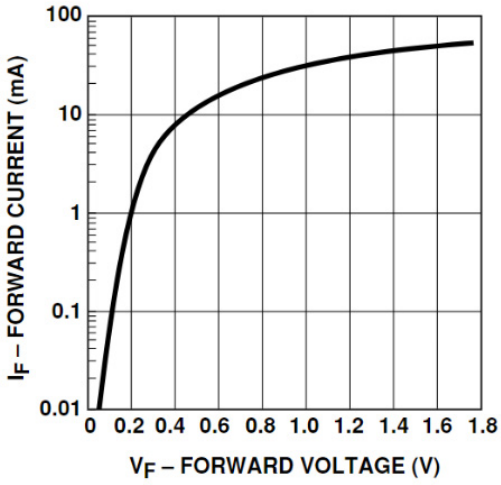

FIGURE 3. Diode characteristic curve V-I [12].

TABLE 2. FR4 epoxy glass design parameters.

Substrate Parameters	Values
Operation frequency	2.45 GHz
Dielectric constant	4.4 (FR-4)
Substrate thickness	1.6 mm
Loss Tangent	0.02

TABLE 3. Antenna dimensions.

Parameters	Dimension by equations (mm)
W	37.26
L	28.8296
W_0	2.9836
y_0	10.6945
n_w	0.1993

order to capture the greatest amount of RF energy in the specified frequency band. Considering the availability of the different materials, FR4 Epoxy Glass material was selected, and their design parameters are characterized in Table 2.

2.2.1. Microstrip Patch Antenna

A 2.45 GHz microstrip patch antenna was designed, it is powered by a microstrip line with insertion which allows to couple the impedance of the patch with the microstrip line to later place a 50 Ω SMA connector. HFSS student version software was used for the simulation of the antenna which allows to study the behavior of different high frequency structures and model them in a simple way. For the microstrip patch antenna design, first the dimensions of the patch (both width W and length L) were calculated, and the width was calculate using Equation 1.

$$W = \frac{V_o}{2f_r}\sqrt{\frac{2}{\epsilon_r + 1}} \tag{1}$$

where V_o is the speed of light, f_r the Resonance frequency (2.45 GHz), and ϵ_r the dielectric constant (4.4). The antenna length was calculate using Equation (2).

$$L = \frac{1}{2f_r\sqrt{\epsilon_{reff}}\sqrt{u_o e_o}} - 0.824h\frac{(\epsilon_{reff}+0.3)(\frac{W}{h}+0.264)}{(\epsilon_{reff}-0.258)(\frac{W}{h}+0.8)} \tag{2}$$

where ϵ_{reff} is the effective dielectric constant, u_o the vacuum permeability, ϵ_o the vacuum permittivity, and h the substrate height (1.5 mm). The dimensions of the 50 Ω power line were found by using the insertion feeding method to couple the patch and the transmission line, which consists of creating a symmetrical insertion to the transmission line of length y_0 from the edge of the patch to its center, with a width of n_w Fig. 2.

Once the dimensions were obtained, the microstrip antenna patch was modeled with the corresponding variables and dimensions, as shown in Table 3.

Finally, an optimization process was carry out with small variation steps of 0.01 mm. To achieve the desired response at 2.45 GHz, the length of the patch L was reduced about 0.06 mm, and the width of the insertion n_w was increased approximately 0.08 mm.

2.2.2. The Rectifier Circuit

A rectifier circuit of type multiplier-rectifier was chosen, and this circuit allows to rectify the signal and obtain a output signal twice the peak voltage of the input signal. This circuit is widely used in energy harvesting devices, formed by two capacitors and two diodes. The HSMS-2850 Schottky diode of Agilent Technologies was selected, which has an activation voltage of 250 mV with a current of 1 mA. This type of diode works in the same way as a normal diode, but differs from another type due its low activation voltage and fast switching time, and the characteristic curve of the V_F vs I_F diode is shown in Fig. 3.

In this type of applications it is important to take into account that the capacitors must have low resistance to avoid energy loss at high frequencies. The chosen capacitors are ceramic MLCCs SMD type for surface mount, and they are from the GQM series and manufactured by muRata Electronics. The capacitor

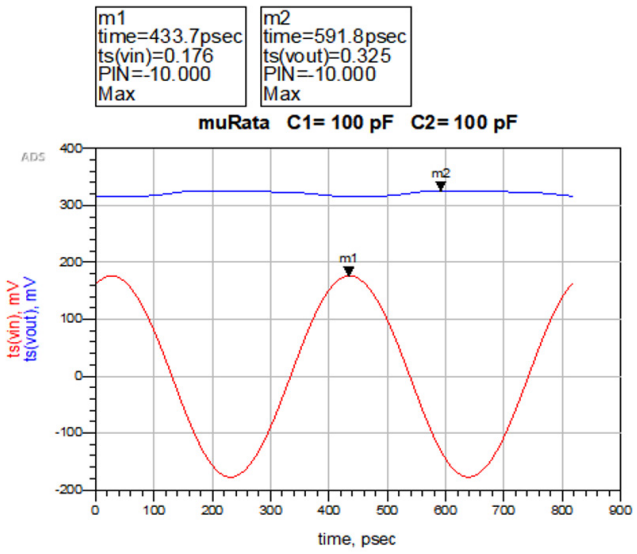

FIGURE 4. Rectifier circuit response, muRata capacitor.

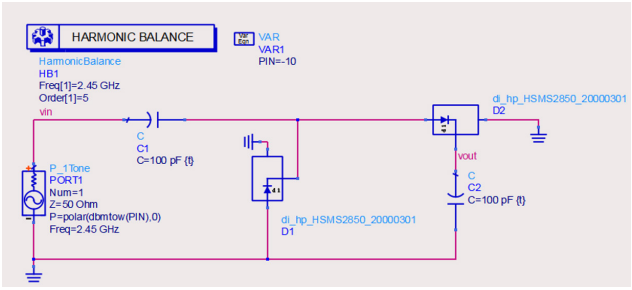

FIGURE 5. Multiplier-rectifier circuit simulation.

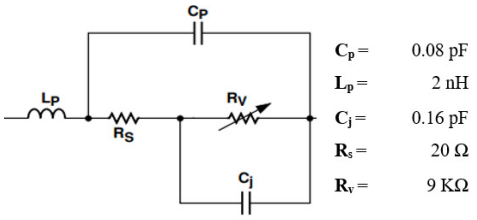

FIGURE 6. Equivalent circuit of the Schottky diode HSMS-2850.

value selection was made using the Tuning tool to find a suitable value. It was defined with a range of values from 1 pF to 1 nF in order to check the response to different capacitor values. The circuit simulation includes the Harmonic Balance module which allows for nonlinear components analysis such as diodes, and the module also allows capturing voltage measurements at input and output of the circuit.

When using a capacitor of 100 pF, it can be observed that the voltage at the output V_out circuit is 0.296 V, and the voltage at the input is $Vin = 0.179$ V (See Fig. 4). Ideally, the multiplier-rectifier circuit should have an output voltage of twice the input voltage. As observed, this result is not achieved because there is no coupling network that allows matching the impedance between the generator and the multiplier-rectifier circuit, so a coupling network is necessary to allow the maximum energy transfer. To obtain a more realistic response from the circuit, the library of muRata capacitors were included. Fig. 4 shows the behavior of the circuit, since it includes all the characteristics of the selected capacitor such as its operating temperature, nominal voltage, operating frequency among others.

Finally, Fig. 5 shows the scheme of the multiplier-rectifier circuit where the Schottky HSMS-2850 diode was used, and their simulation parameters are available in professional software and specifically at the library for high frequency diodes. Also, an AC power source was used to simulate the signal that the receiving antenna will pass to the rectifier circuit, and it is configured in the frequency of 2.45 GHz with an impedance of 50 Ω and an initial power value of −10 dBm.

2.2.3. Coupling Network

The proposed coupling network was designed in order to couple the output impedance of 50 Ω antenna to the input impedance of the multiplier-rectifier circuit. To achieve this, it was necessary to calculate the impedance of the multiplier-rectifier circuit. In this case, the equivalent circuit of the Schottky diode HSMS-2850 provided by its datasheet is used to find the exact impedance of the circuit as shown in Fig. 6.

The resulting circuit is shown in Fig. 7 where the S-parameters module was used to determine the dispersion parameters. A terminal was included to indicate the impedance to which it is required to couple, and in this case it is 50 Ω. The S_{11} parameter was plotted in a Smith chart to determine the impedance. In this case at the frequency of 2.45 GHz, a normalized impedance value of $Z_0 * (0.170 - j2.417)$ was observed, and when $Z_0 = 50\,\Omega$, there is an input impedance value of $Z_{in} = 8.509 - j120.838$.

Once the impedance at the input of the multiplier-rectifier circuit was found, the Smith chart tool and its module were used. To design the coupling network, the load impedance was defined corresponding to the calculated impedance $Z_L = 8.509 - j120.838\,\Omega$ and the source impedance corresponding to the impedance at the output of the antenna $Z_{source} = 50\,\Omega$. For this design, distributed elements or sections of transmission lines were used for the coupling network, due to its easy implementation with microstrip technology. To consider the energy storage stage, the impedance value must be calculated again taking into account the value of the capacitor used.

2.2.4. Energy Storage Stage

To complete the simulation of the circuit, it was necessary to add at the output of the rectifier circuit a stage that allows to store the energy, which was done by introducing a capacitor C_L together with a parallel resistor R_L. Due to this addition, the capacitor C_L and resistor R_L were included to recalculate the impedance value, and thus determine the coupling network used in the final circuit as shown in Fig. 7.

The new impedance value including the energy storage stage is $Z_0 * (0.1702 - j2.4145)$, and when $Z_0 = 50\,\Omega$ there is an input impedance value of $Z_{in} = 8.5095 - j120.7266$. The values of $C_L = 220$ pF and $R_L = 10$ kΩ were determined by the Tuning tool. Observing the behavior of the circuit, the

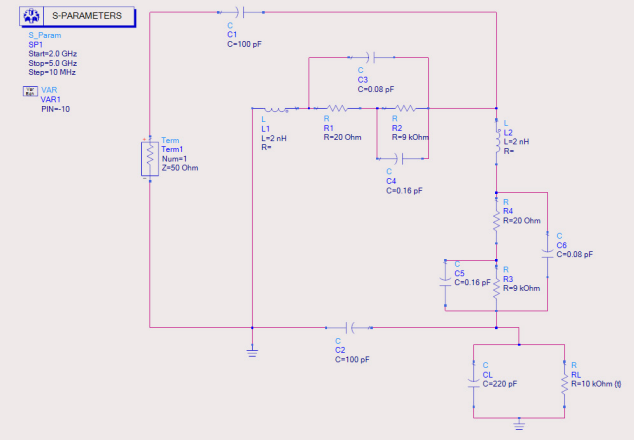

FIGURE 7. Rectifier circuit with energy storage stage.

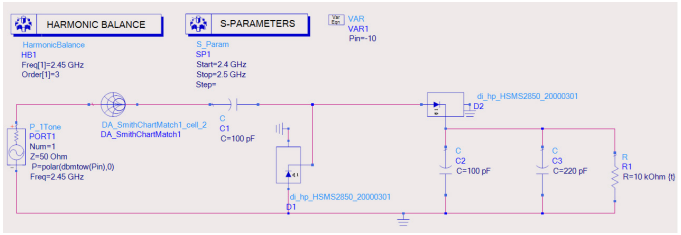

FIGURE 8. Circuit design including smith chart.

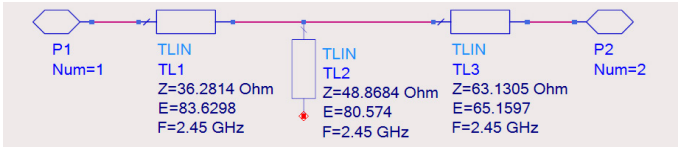

FIGURE 9. Coupling network design.

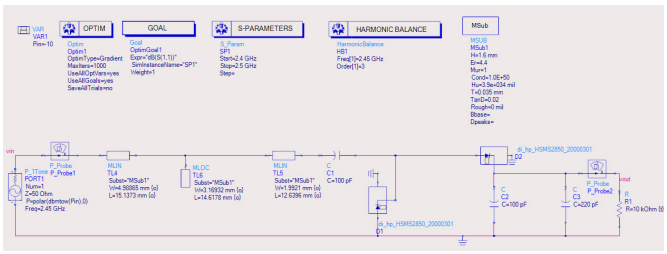

FIGURE 10. Final circuit design.

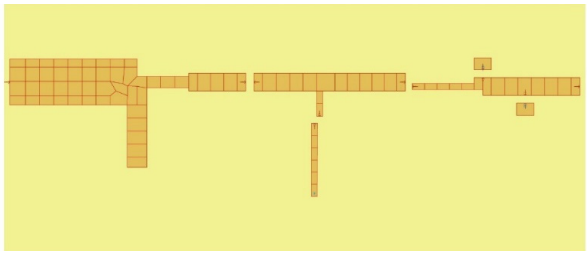

FIGURE 11. Final layout of the rectifier.

R_L allows the C_L capacitor to discharge, and the C_L capacitor allows smoothing the output signal.

In the coupling network design, the load impedance was defined corresponding to the new calculated impedance $Z_L = 8.509 - j120.838\,\Omega$ and the impedance of the source corresponding to the impedance at the output of the antenna defined as $Z_{source} = 50\,\Omega$, see Fig. 8. The software has three components for distributed elements that could be used in the design of the coupling network, which are: transmission lines, open stubs, and shorted stubs. In this case, transmission lines and open stubs were used. They allowed the impedance to be coupled until reaching $50\,\Omega$. It must be considered that the coupling network must maintain a bandwidth; therefore, the curves Q or quality factor were used; in this case, the different sections of lines were entered, keeping them within the curve Q until reaching $50\,\Omega$. Once the coupling network was designed in the Smith chart tool, the circuit was exported through the Smith chart block, which has inside the design of the coupling network as shown in Fig. 9.

The components in Fig. 9 are given by their characteristic impedance (Z_0) and electrical length (E), which were transformed to physical dimensions of width (W) and length (L) for later implementation, and this transformation was carried out by the LineCalc tool Then, the Smith chart block was replaced by the coupling network in physical dimensions as shown in Fig. 10, and the final circuit for the RF energy harvesting device was obtained. The P_Probe components and the V_{in} and V_{out} pins were included to perform the corresponding circuit tests.

To generate the final layout, it was necessary to make a series of considerations (see Fig. 11) that were added to the circuit to be implemented later. These considerations were,

1. MTEEs were placed in the places in which three lines of different widths meet and MSTEPs in the places in which two lines with different widths meet. This aims to eliminate discontinuities that alter the behavior of the circuit.

2. MGAP was added, which allows defining the space between the lines leaving enough space to place both the capacitors and Schottky diodes according to their dimensions.

3. VIAGND was added to simulate the effect of ground connections, and the diameter of the hole that is made to connect it to the ground plane.

4. New lines were added and allowed the connections of the different components considering their space and the place in which each of them was welded.

To verify that the circuit is working properly, an electromagnetic simulation was perform, in which both the circuit design and the electronic components were considered (capacitors and Schottky diodes), for which, the ports, the substrate used, and the frequency plan were defined; in addition, the Momentum Microwave simulation type was selected.

Once the simulation of each stage verified the proper operation of each stage of the device, both the microstrip patch antenna and the rectifier circuit were manufactured as shown in

Table 4. WiFi router operation features.

Characteristics	Value
WiFi Channel	11
Center Frequency	2.462
Frequency Range	2.451–2.473
RF Transmition Power	20 dBm

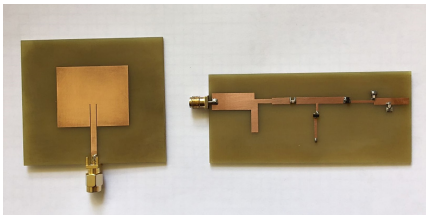

FIGURE 12. Antenna and rectifier circuit manufactured.

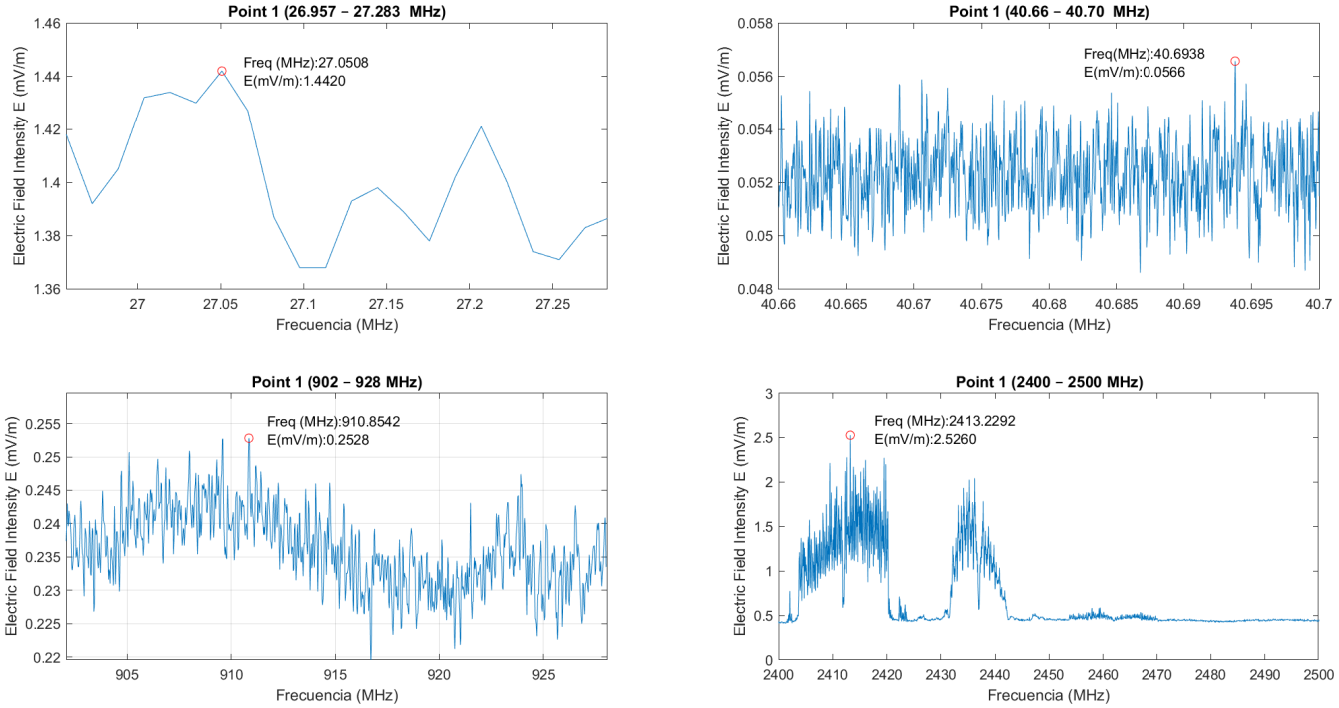

FIGURE 13. Field strength at the first point.

Fig. 12. The power conversion efficiency (PCE) was evaluated using Eq. (3) [16]:

$$PCE(\eta) = \frac{V_{out}^2}{P_{in} \times R_L} \times 100\% \tag{3}$$

3. RESULTS

The results are organized into four sections. First, the spectrum measurements are presented, followed by the microstrip patch antenna measurements. Subsequently, the rectifier circuit measurements are discussed, and finally, the measurements of the entire EH device are presented.

3.1. Spectrum Measurements

The measurements were obtained using the NARDA SRM 3006 equipment at various locations, encompassing the operational frequencies of both the equipment and the antenna available in the laboratory. These frequencies include the ranges of 26.957–27.283 MHz, 40.66–40.70 MHz, 902–928 MHz, and the band of 2400–2500 MHz. Subsequently, the data stored within the equipment were extracted utilizing the SRM-3006 Tools software and were graphed using mathematical software. As an illustrative example, the results of measurements conducted at the initial point for the different frequencies under study are presented in Fig. 13. It is clear to see that the higher electromagnetic field is received at 2.4 GHz band with a peak of 2.526 mV/m. Through an examination of all the measurements conducted within the ISM band, specific attention is given to the 2.4 GHz ISM band in which the higher electromagnetic field is received.

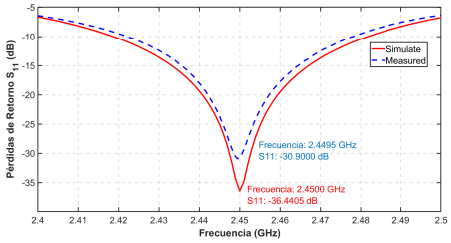

FIGURE 14. Antenna return loss simulate vs measurement.

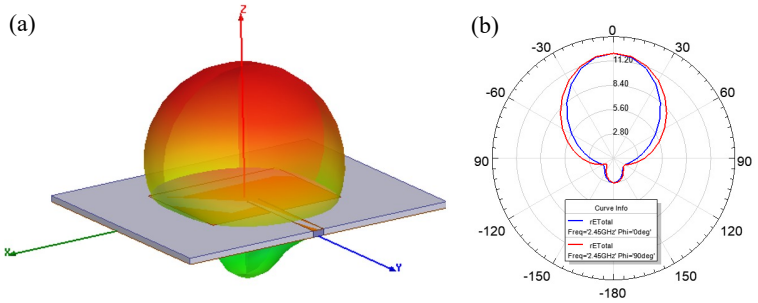

FIGURE 15. Microstrip patch antenna radiation pattern. (a) 3D antenna radiation pattern. (b) Radiation pattern blue $\phi = 0$ (E plane) and red $\phi = 90$ (H plane).

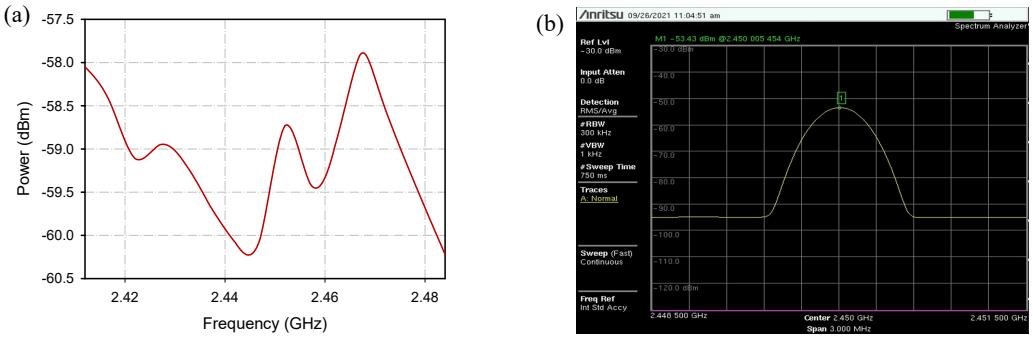

FIGURE 16. Rectifier circuit evaluation. (a) Received power levels on WiFi channels with the design microstrip patch antenna. (b) Power level received by the antenna at 2.45 GHz.

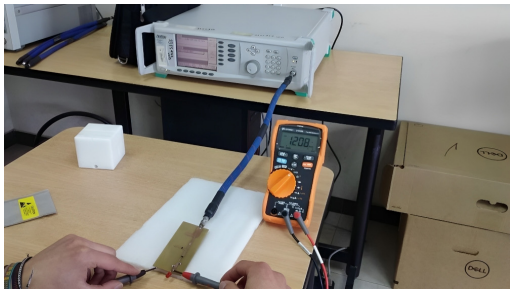

FIGURE 17. Measurements setup for output Voltage vs Input Power for the rectifier circuit

3.2. Microstrip Patch Antenna Measurements

The measurements of the microstrip patch antenna were obtained using the final design, which incorporates the optimized dimensions outlined in Table 3. An important parameter evaluated was the S_{11} parameter, also known as return losses, which quantifies the power reflected by the antenna. As shown in Fig. 14, the antenna resonates at a frequency of 2.45 GHz and exhibits a return loss of -36.44 dB. Furthermore, the antenna's bandwidth below -10 dB spans from 2.4187 GHz to 2.4817 GHz, resulting in a bandwidth of approximately 63 MHz. In Fig. 15, radiation pattern is shown, in which a gain of 3.6947 dB was obtained in the maximum radiation direction.

Fig. 16(b) shows the received power P_{RX} at the frequency of 2.45 GHz (in the maximum radiation direction) resulting in a value of $P_{RX} = -53.43$ dBm. These measurements were perform with the spectrum analyzer ANRITSU model MS2724C. Also, measurements at the antenna were carried out for different frequencies considering the central frequencies of the different WiFi channels, and these measurements can be seen in Fig. 16(a).

3.3. Rectifier Circuit Measurements

Measurements for different input powers and the corresponding rectified voltage at the output were performed to verify the device's ability to harvest RF energy. A signal generator ANRITSU model MG3692C center at 2.45 GHz was used, and the power was varied from -20 dBm to 20 dBm with 2 dB steps, as shown in Fig. 17.

In Fig. 18(a), the output voltage vs input power at the rectifier is shown. Also, in Fig. 18(b) the Power Conversion Efficiency (PCE) as presented in [16] (i.e., as a function of the input power

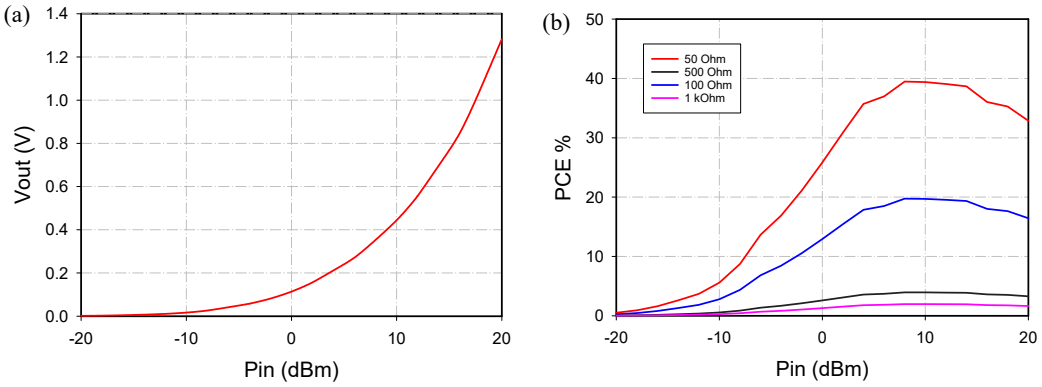

FIGURE 18. Rectifier circuit evaluation. (a) Measured V_{out} vs P_{in} of rectifier circuit. (b) PCE vs. Pin with different load values.

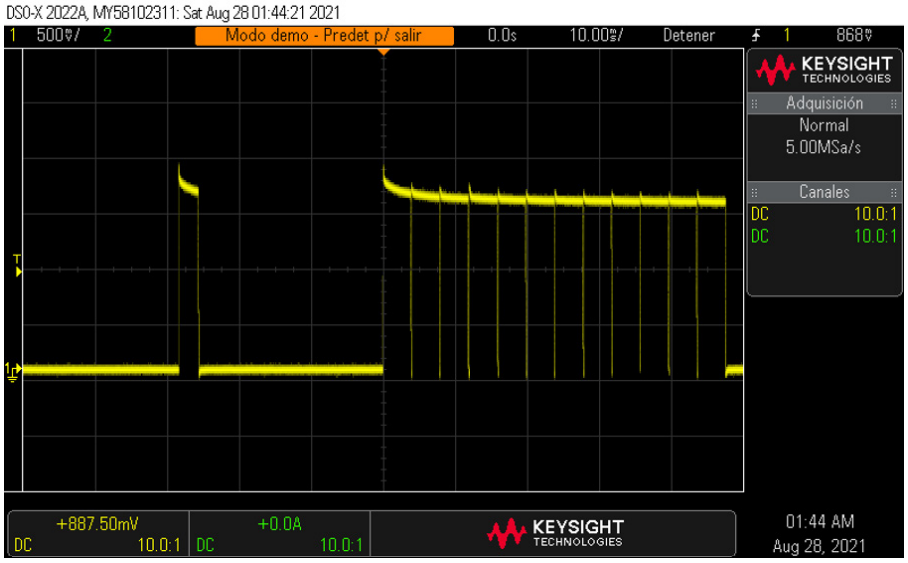

FIGURE 19. Power harvesting with device connected to router.

(P_{in}) at various load resistance values) is shown. Because the rectifier was designed for 50 Ω load impedance, the maximum PCE of 40% wwa obtained with 50 Ω load.

The rectifier's output was also observed using an oscilloscope. In this scenario, an RF (AC) signal was generated with a signal generator and fed into the input of the rectifier circuit at a power level of approximately 20 dBm and a frequency of 2.45 GHz. To validate the rectifier's operation, a red LED diode with a threshold voltage of 1.6 V was connected to its output. The LED illuminated when the rectifier circuit was provided with a power input of around 25 dBm, confirming its functionality.

3.4. Device Measurements

To verify the ability of the device to harvest RF energy, a WiFi router was used in its default configuration with the characteristics shown in Table 4. Any router or AP periodically sends a signal known as "beacon", which contains information about the connection and allows devices to recognize network characteristics. These signals are sent every 40 to 1000 ms, but by default set to 100 ms. An oscilloscope was used to observe the signal at the output of the RF energy harvesting device.

When harvesting energy from the WiFi router without having traffic on the network, the only signal that is captured corresponds to the "beacon" that is sent every 100 ms. It is necessary that the network remains in use to be able to capture more energy from WiFi radio waves, due to the dynamic behavior of the signal. In this way, the signal can remain constant when sending more packets as shown in Fig. 19. The voltage measured at the output of the Electromagnetic Harvesting device was 510.6 mV or 0.51 V, measured with the rectenna at a distance from the WiFi modem about 10 cm.

4. CONCLUSIONS

Through field strength measurements carried out within the Facultad de Informatica y Electronica, it was concluded that the 2.4 GHz ISM band is the one with the highest levels of field strength. For this reason, there is a better opportunity for the harvesting of RF energy.

The microstrip patch antenna and the rectifier circuit at 2.45 GHz were designed, and a return loss of −30.9 dB, a

VSWR of 1.12, and a bandwidth of around 56 MHz were obtained. Therefore, it was concluded that the antenna is coupled, and the return losses are minimal. However, due to the utilization of a dielectric substrate with a high loss tangent, the antenna efficiency is limited, and a value of 0.46 is obtained by simulation.

The diode as a nonlinear element, therefore, throughout the rectification process of the AC signal several harmonics could be produced, which reduces the amount of DC at the output of the device. The harmonic balance method was used for its study, where the level of the signal in DC (0 Hz) obtained by simulation is 4,032 dBm for an RF input signal of 2.45 GHz with a power of −10 dBm. Also it was determined that the RF component in the output at the fundamental frequency (2.45 GHz) is attenuated at 29.87 dBm, achieving the rectification of the signal.

The continuous voltage measured at the output of the rectifier circuit for different power values configured in the RF signal generator gave different results as follows: for 0 dBm it was measured 113.3 mV, for 10 dBm 443.8 mV, and for 20 dBm 1282 mV. In addition, the radio frequency energy generated by a WiFi router was harvested at 10 cm with a measured voltage of 510.6 mV. The rectified signal was displayed on the oscilloscope and the operation verified by turning on an LED diode with a threshold voltage 1.6 V.

The designed rectenna for a radio frequency energy harvesting system has a useful performance by harnessing RF waves available in the environment, and this rectenna could provide a consistent source of energy, resulting in reduced reliance on conventional batteries and increased autonomy in low-power electronic devices which work with an small amount of voltage level. This enables the ability to operate in environments where energy is scarce or intermittent such as the Internet of Things and self-powered RFID tags. Also, compared to other energy sources, radio frequency sources have no limitations in both space and time, including mobile communications, radio and television broadcasting, WiFi networks among other technologies that are widely used.

REFERENCES

[1] Priya, S. and D. Inman, *Energy Harvesting Technologies*, vol. 21, 2, Springer, New York, USA, 2009.

[2] Brown, W. C., "The history of the development of the rectenna," *Energy*, 1980.

[3] Sidhu, R., J. Singh Ubhi, and A. Aggarwal, "A survey study of different rf energy sources for rf energy harvesting," in *2019 International Conference on Automation, Computational and Technology Management (ICACTM)*, 530–533, 2019.

[4] Canas Encinas, R. and A. Aggarwal, "Transferencia inal'ambrica de energia," *Univ. Pol*, 2015.

[5] Glaser, P. E. and O. Maynard, "Solar power via satellite," *Fundamental and Applied Aspects of Nonionizing Radiation*, 433–446, Springer, Boston, MA, US, 1973.

[6] Srinivasu, G., V. Sharma, and N. Anveshkumar, "A survey on conceptualization of rf energy harvesting," *Journal of Applied Science and Computations (JASC)*, Vol. 6, No. 2, 791–800, 2019.

[7] Mart'inez Castillo, A. and N. Anveshkumar, "Antenas para aplicaciones de captacion de energia en la banda uhf," *Univ. Pol. Valencia*, 2014.

[8] Wagih, M., A. Weddell, and S. Beeby, "Rectennas for radio-frequency energy harvesting and wireless power transfer: a review of antenna design [antenna applications corner]," *IEEE Antennas and Propagation Magazine*, Vol. 62, No. 5, 95–107, Oct. 2020.

[9] Prieto Poyatos, A. and S. Beeby, "Diseno de un sistema de captacion de energia de senales wifi," *Telecomunicacion*, 2019.

[10] Silijestrom, P. and S. Beeby, "Diseno de una rectenn en la banda wifi de 2.45 ghz para aplicaciones de captacion de energia electromagnetica," *Universidad Politecnica De Cartagena*, 1–74, 2015.

[11] Saffari, P., A. Basaligheh, and K. Moez, "An rf-to-dc rectifier with high efficiency over wide input power range for rf energy harvesting applications," *IEEE*, Vol. 66, No. 12, 4862–4875, 2019.

[12] Tran, L.-G., H.-K. Cha, and W.-T. Park, "Rf power harvesting: a review on designing methodologies and applications," *Springer*, Vol. 5, 1–16, 2017.

[13] Divakaran, S., D. Krishna, and Nasimuddin, "Rf energy harvesting systems: an overview and design issues," *Wiley Online Library*, Vol. 29, No. 1, e21633, 2019.

[14] Reed, R., F. Pour, and D. Ha, "An efficient 2.4 ghz differential rectenna for radio frequency energy harvesting," in *63rd IEEE International Midwest Symposium on Circuits and Systems (MWSCAS)*, 208–212, electr Network, Apr. 09-12, 2020.

[15] Huang, Y., N. Shinohara, and H. Toromura, "A wideband rectenna for 2.4 ghz-band rf energy harvesting," in *2016 IEEE Wireless Power Transfer Conference (WPTC)*, aveiro, Portugal, May 05-06, 2016.

[16] Dey, A., N. Semwal, and W. Arif, "Design of a compact and efficient 2.4 ghz rectenna system for energy harvesting," *Journal of Electromagnetic Waves and Applications*, Vol. 36, No. 13, 1850–1868, Sep 2, 2022.

[17] D'mello, S. and W. Arif, "Study of ism band technologies," *Iosr Journal of Engineering*, Vol. 8, 35–39, 2018.

[18] Packard, H. and W. Arif, "Surface mount microwave schottky detector diodes," *Technical Data*, 1999 .

[19] Meher, P., S. Mishra, and M. Halimi, "A low-profile compact broadband cp dra for rf energy harvesting applications," *Iete Journal of Research*, Jul. 27, 2023.

[20] International Telecomunication Unit, "Radio regulations articles: Edition of 2020", Geneva, 2020.